SUPPLEMENTARY FIGURE LEGENDS

Supplementary Table 1. Genetic interactions between Ral^{35d} and autophagy gene hypomorphs, Related to Figure 1.

Females carrying a scaGAL4 transgene and the Ral^{35d} hypomorphic mutation were crossed with males carrying dsRNA-expressing transgenes targeting the genes indicated in column 1. The loss-of-bristle phenotype of Ral^{35d} males (control) and of Ral^{35d} males expressing the indicated dsRNA under the control of scaGAL4 was analyzed. The distribution of phenotypes in each genetic context is shown. Each distribution was compared to the control distribution using a Chi-Square Goodness-of-Fit test. All distributions are significantly different from control (p value<10E-4), with the exception of dsATG2 (p value=0.48). No bristle phenotype was observed in flies expressing the dsRNAs in absence of Ral^{35d}. Similar genetic interactions were observed when a dominant negative allele of Ral (Ral^{S25N}) was used instead of the Ral^{35d} mutant used here (data not shown).

Supplementary Figure 1: RalB and an Exo84-containing subcomplex of the exocyst are necessary for amino acid starvation induced autophagy, Related to Figure 2.

A: Validation of siRNA mediated protein depletion. Hela cells stably expressing GFP-LC3 were depleted of the indicated proteins by siRNA transfection. Western blots were performed to confirm protein knockdown.

B: Depletion of RalGAPβ activates RalB. Endogenous GTP-bound RalB was collected by GST-Sec5-RBD mediated affinity purification from HEK-293 cells incubated in DMEM or EBSS for 4 hours and visualized with specific anti-RalB antibody.

C: RalGAP depletion induces accumulation of GFP-LC3 punctae. Hela cells stably expressing GFP-LC3 were depleted of the indicated proteins by siRNA transfection. Cells were cultured in Opti-MEM I (Invitrogen) plus 5% FBS for 24 hours before imaging to reduce the baseline level of autophagy. Cells were imaged by GFP fluorescence 96 hours after transfection.

D: RalGAP depletion induces accumulation of GFP-LC3 punctae. GFP-LC3 punctae in cells treated as in (C) were quantitated. The mean distribution of GFP-LC3 punctae/cell is displayed as a bar graph, data are represented as mean +/- SEM. P-values were calculated by one-way ANOVA followed by Dunnett's Multiple Comparison Test.

E: Inhibition of GFP-LC3 punctae correlates with accumulation of LC3 protein. The mean total intensity of GFP-LC3 in cells treated as in (A) was quantitated. The distribution of the mean total GFP intensity is displayed as a bar graph. P-values were calculated by one-way ANOVA followed by Dunnett's Multiple Comparison Test.

Supplementary Figure 2: Nutrient deprivation drives assembly of Exo84/Beclin1 complexes, Related to Figure 4.

A: Exo84 and Sec5 both require amino acids 88-150 of Beclin1 to associate with Beclin1. Expression constructs for Myc-Exo84 (left panel) or HA-Sec5 (right panel) were co-transfected into HEK-293 cells together with the indicated Beclin1 deletion mutants. 48 hours post transfection the indicated proteins were immunoprecipitated with antibodies directed to the specified tag. Immunoprecipitates were analyzed for coprecipitation with the indicated Flag-Beclin1 deletion mutants. Arrow indicates minor cross reactivity with IgG heavy chain. Whole cell lysate (WCL), Immunoprecipitates

(IP).

B: Sec5 and Exo84 partition into distinct high molecular weight fractions. Detergent soluble extracts from MDCK cells were separated by FPLC on a Superose 6 column. The fractions were analyzed for Sec5, Exo84, Beclin1, ULK1, and RalB. The position of molecular weight markers are indicated (Thyroglobulin 669 kDa, Apo-Ferritin 440 kDa, Catalase 232 kDa, and Bovine serum albumin 67 kDa).

C: Sec5 co-localizes with golgi marker GM130. Endogenous immunofluorescence of Sec5 (anti-Sec5) and GM130 (anti-GM130) in MDCK cells. Dashed lines indicated cell borders as visualized in a saturated exposure. Scale bar 10µm.

Supplementary Figure 3: Active ULK1 associates with Exo84, Related to Figure 7.

A: ULK1 requires amino acids 244-337 of Beclin1 to associate with Beclin1. Expression constructs for HA-ULK1 were co-transfected into HEK-293 cells together with the indicated Beclin1 deletion mutants. 48 hours post transfection the indicated proteins were immunoprecipitated with antibodies directed to the HA tag. Immunoprecipitates were analyzed for coprecipitation with the indicated Flag-Beclin1 deletion mutants. Whole cell lysate (WCL), Immunoprecipitates (IP). $IP_{Beclin1}$ to IP_{ULK1} ratios were calculated by division of quantified Beclin1 signal by the ULK1 signal from the same sample.

B: Sec5 but not Exo84 associates with mTORC1. Expression constructs for Myc-Exo84 or HA-Sec5 were transfected into HEK-293 cells as indicated. 48 hours post transfection the indicated proteins were immunoprecipitated with antibodies directed to the specified tag. Immunoprecipitates were analyzed for coprecipitation with endogenous mTORC1 components mTOR (left and right panels) and Raptor (right panel only). Two

independent experiments are shown. Whole cell lysate (WCL), Immunoprecipitates (IP).

C: ULK1/Exo84 complexes accumulate during extended Rapamycin exposure but are not responsive to short term mTOR inhibition (1 hour Rapamycin). Co-expression, co-IPs with the indicated proteins were performed as in (A) with the addition of exposure to 50nM Rapamycin or 0.1% DMSO vehicle for the indicated times before immunoprecipitation.

D: Beclin1/Sec5 complexes are dissociated during extended Rapamycin exposure but are not responsive to short term mTOR inhibition mTOR inhibition (1 hour Rapamycin). Co-expression, co-IPs with the indicated proteins were performed as in (C).

SUPPLEMENTAL MATERIALS AND METHODS

Plasmids. GFP-Sec3 and GFP-Sec10 (Matern et al., 2001), GFP-RalB (Cascone et al., 2008), Flag-RUBICON and Flag-ATG14L (Zhong et al., 2009), Myc-RLIP76 (Rosse et al., 2003), Myc-Rlip(RBD) (Moskalenko et al., 2002), Myc-Exo84 (Moskalenko et al., 2003), Myc-rSec5 and Myc-rSec5(T11A) (Spiczka and Yeaman, 2008), Myc-Sec8 and HA-Sec5 (Moskalenko et al., 2002), Flag-Beclin1 (Pattingre et al., 2005), GFP-ATG5 (Mizushima et al., 2001), GFP-2X-Fyve (Vieira et al., 2001), GFP-LC3 (Mizushima et al., 2004), Monomeric RFP-LC3 (Bampton et al., 2005), Flag-RalB, Flag-RalB(G23V), Flag-RalB(G23V, E38R), Flag-RalB(G23V, A48W), Flag-RalB(E38R), and Flag-RalB(A48W) (Cascone et al., 2008), Flag-Vps34 (Liang et al., 2006), and HA-ULK1 and HA-ULK1(K46N) (Okazaki et al., 2000) were previously described.

Antibodies. Rabbit anti-GFP (sc-8334), Mouse anti-c-Myc (sc-40), Rabbit anti-HA (sc-805), Rabbit anti-ATG5 (sc-33210), Goat anti-Beclin1 (sc-10087), and Rabbit anti-Myc (sc-789) were purchased from Santa Cruz Biotechnology, inc. Rabbit anti-Flag (#F2555) and Mouse anti-Flag (#F1804) were purchased from Sigma-Aldrich, inc. Rabbit anti-VPS34 (#382100) was purchased from Invitrogen. Rabbit anti-ULK1 (#AP8104d) and Rabbit anti-UVRAG (#AP1850e) were purchased from Abgent, inc. Mouse anti-RalA (#3526) and Rabbit anti-Beclin1 (#3738) were purchased from Cell Signaling Technology, inc. Rabbit anti-ATG14L (#PD026) and anti-LC3 (#PM036) were purchased from Medical & Biological Laboratories Co. Mouse anti-RalB was provided by Larry Feig, Tufts University. Mouse and Rabbit anti-Exo70, Exo84, Sec3, Sec5, Sec6,

Sec8, and Sec15 were provided by Charles Yeaman (Hsu et al., 1996; Kee et al., 1997; Yeaman, 2003). Rabbit anti-Sec10 (#17593-1-AP) was purchased from ProteinTech Group, Inc.

Immunofluorescence. Cells on coverslips were fixed in 3.7% formaldehyde in PBS for 15 minutes. Coverslips were rinsed twice in PBS, quenched in 50mM NH_4Cl in PBS for 15 minutes, rinsed twice in PBS, then permeabilized in 100µg/mL digitonin in PBS for 10 minutes on ice (Exception anti-RalA samples were permeabilized 5 minutes in -20ºC acetone). Coverslips were rinsed twice in PBS and blocked in 2% BSA in PBS for 30-60 minutes at 37ºC followed by incubation with primary antibodies diluted in 2% BSA in PBS for 1-2.5 hours at 37ºC. Coverslips were then washed four times for 5 minutes in PBS and incubated with secondary antibodies diluted in 2% BSA in PBS for 1-1.5 hours at 37ºC. Coverslips were then washed four times for 5 minutes in PBS. Coverslips stained with two primary antibodies, were subsequently stained with a second primary-secondary antibody combination. Coverslips were mounted on glass slides with either ProLong Gold mounting medium (Invitrogen) or Vectashield fluorescent mounting medium (Vector Labs). Secondary antibodies: DyLight 488 Donkey anti-Rabbit and DyLight 594 Donkey anti-Mouse were puchased from Jackson ImmunoResearch Laboratories, inc. Alexa Fluor 350 Donkey anti-Mouse and Alexa Fluor 647 Donkey anti-Mouse were purchased from Invitrogen.

Image capture and quantitation. Epifluorescence images (Figure 1I, 1L) were captured using appropriate excitation/emission filter sets(GFP, AlexaFluor 488) (Rhodamine,

AlexaFluor 594) on a 40X objective on a Zeiss Axioplan 2E**.** Deconvolution confocal images (Figure 1J, 1N, 2A, 2F, 3A-3F, 6G, and Supplementary Figure 2C) were captured using appropriate filter sets (DAPI Excitation: 360/40, Emission: 457/50; FITC, Excitation: 490/20, Emission 526/38; TRITC Excitation: 555/28, Emission 617/63; Cy5 Excitation: 640/20, Emission: 685/40) and the 60X objective on an Applied Precision personal DV deconvolution microscope. Deconvolution confocal images of cells were captured as Z-section stacks and the stacked images underwent 10 iterations of restorative deconvolution. In Figure 1K, cellular fluorescence intensity was quantified by ImageJ. Briefly, cells were encircled using the freehand selection tool, each cell was saved as a region of interest, and the total fluorescence of each region of interest was measured for both FITC (anti-LC3) and TRITC (anti-Myc) channels using the measure function. In Figures 1M, 1O, 2D, 6H, 6I, and Supplementary Figure 2D images were blinded, mixed, and scored for punctae by the author. In Figure 2B and 2F, punctae were quantified in ImageJ. Briefly, images were background subtracted, then thresholds were optimized to differentiate negative control (siControl) and positive control (siAtg5) samples. The analyze particles function of ImageJ was utilized to quantitate punctae for all samples under identical conditions. Finally, the number of punctae per cell was calculated by division of the total punctae per field divided by the number of nuclei per field. In Figure 2C and Supplementary Figure 2E, mean total fluorescence was calculated in ImageJ. Briefly, cells were selected in the GFP channel using the freehand selection tool and saved as regions of interest. Then, the mean fluorescence of each region of interest was measured in the GFP channel using the measure function.

Immunoprecipitation and immunoblotting. 5 X 10^5 HEK293 cells were seeded into 35mm dishes 18-24 hours before transfection. 500ng of each plasmid was transfected with Fugene 6 at a ratio of 3:1 (µL Fugene 6 to µg DNA) in to 2mL 10% FBS DMEM-H. 18-24 hours later the media was replaced with 2mL 10%FBS DMEM-H. For nutrient stimulation/starvation assays, the cells were then incubated as described with 2mL serum free DMEM-H or EBSS for the times described. The cells were lysed in lysis buffer (20 mM Tris-HCl pH 7.4, 137mM NaCl, 1% Triton-X-100, 0.5% Sodium Deoxycholate, 10mM $MgCl_2$, 2mM EGTA) plus protease and phosphatase inhibitors (Roche EDTA-free protease inhibitor cocktail, 1mM PMSF, 50mM NaF, 1mM $NaVO_4$, 80mM β-glycerosphosphate). Cells were lysed for 15 minutes, then cleared at 20,000 X g for 10 minutes at 4ºC. 800µg of lysate was diluted with lysis buffer to a concentration of 1µg/µL. Complexes were immunoprecipitated with 2µg of the indicated antibody for an empirically derived period ranging between 2 to 16 hours. Antibody-antigen complexes were precipitated with ProteinA/G-agarose beads for 1 hour. Complexes were washed in lysis buffer 3-4 times for 5 minutes at 4ºC. Samples were subsequently separated by SDS-PAGE and transferred to Immobilon-P polyvinylidene (PVDF) membranes. Ral-GTP pulldowns were performed as described previously (Chien et al., 2006). Immunoblot analysis was performed with the indicated antibodies and visualized with SuperSignal West Pico Chemiluminescent substrate (Pierce Chemical).

Coimmunoprecipitation kinase assay. Immunoprecipitates were prepared as described above. After the final wash in lysis buffer, the beads were rinsed 3 times in 1X Reaction buffer (25 mM MOPS pH 7.5, 1mM EGTA, 0.1mM Sodium Vanadate, 15mM $MgCl_2$, 5

mM β-glycerol phosphate). Then 30µL of reaction buffer containing 1mg of myelin basic protein (MBP) and 100µM ATP [10µCi γ-^{32}P-ATP] was added to the beads to initiate the reaction. The reaction proceeded for 1 hour at 30ºC with intermittent shaking to mix the beads. The reaction was terminated by adding 6X laemmli SDS sample buffer and boiling.

***Salmonella typhimurium* Infection.** GFP-expressing *Salmonella typhimurium* (obtained from Mary O'Riordan, University of Michigan (Radtke et al., 2007)) were grown overnight in LB medium at 37ºC, shaking and back-diluted 1:100. When bacteria reached exponential phase, they were washed twice with PBS and used to infect Hela and HBEC30 cells at a multiplicity of infection 10 for 1 hour. Cells were then washed 3 times with PBS and incubated in medium containing 100µg/mL gentamicin for 2 hours. Cells were then washed 3 times with PBS and incubated in medium containing 5µg/mL gentamicin for 1 hour. Cells were then fixed and processed for immuno-fluorescence.

Superose 6 FPLC. MDCK cells were grown to confluence on 15 cm dishes. Cells were washed 1X with HDF before adding EBSS for 90 minutes. Cells were washed two times before lysis in DHE buffer (20mM HEPES, 150mM NaCl, 0.5% NP40, and the protease inhibitors Pefabloc, Antipain, Leupeptin, and Pepstatin A). Collected lysates were incubated on ice for 20 min, then cleared at 20,000 X g for 10 minutes at 4ºC. The supernatant was filtered through 0.22um filter and 0.5mL of filtered sample was injected into a Superosoe 6 column. The column was run at a flow rate of 0.2mL/min and 0.5mL fractions were collected. The collected samples were mixed wiht 100µL 6X laemmli

sample buffer and boiled.

Fly genetic methods

sca-GAL4 flies were provided by F. Schweisguth and *Sec5* and Sec6 mutants were gifts of T. Schwarz. Other mutants were provided from Bloomington and Szeged stock centers. UAS-ds transgenic strains were provided by the Vienna Drosophila RNAi Center (VDRC) (Dietzl et al., 2007). The w^{1118} strain was used as a wild-type stock. Genetic interactions were performed using methods previously described (Balakireva et al., 2006; Rorth, 1998). For each genotype, at least 100 flies were examined and distributed into 4 classes according to their microchaete numbers: flies with no missing microchaetes ("wild-type"), with 1 to 10 ("weak"), 11 to 30 ("middle"), and >30 absent microchaetes ("strong"). Distributions were compared using a Chi-Square Goodness-of-Fit test.

siRNA sequences.

siControl oligos used were siGenome Non-targeting siRNA Pool #1 (Dharmacon Catalog #D-001206-13-05). Single oligos were used to deplete RalA (Figure 2F,G), RalB (Figure 2F,G), Sec5, Sec6, and Exo84:

5'-GACAGGUUUCUGUAGAAGAdTdT-3' (RalA)

5'-GGUGAUCAUGGUUGGCAGCdTdT-3' (RalB)

5'-GGUCGGAAAGACAAGGCAGdTdT-3' (Sec5)

5'-GGGAAGAGAAAAUUGACAGdTdT-3' (Sec6)

5'-GCCACUAAACAUCGCAACUdTdT-3' (Exo84)

siGenome pools were purchased from Dharmacon were used to deplete ATG5, Beclin1,

ULK1, RalA (Figure 2A-C), RalB (Figure 2A-C), Exo70, Sec3, Sec8, Sec10, and Sec15:

ATG5:

5’-GGAAUAUCCUGCAGAAGAA-3’

5’-CAUCUGAGCUACCCGGAUA-3’

5’-GACAAGAAGACAUUAGUGA-3’

5’-CAAUUGGUUUGCUAUUUGA-3’

Beclin1:

5’-CUAAGGAGCUGCCGUUAUA-3’

5’-GGAUGACAGUGAACAGUUA-3’

5’-UAAGAUGGGUCUGAAAUUU-3’

5’-GCCAACAGCUUCACUCUGA-3’

ULK1:

5’-CCUAAAACGUGUCUUAUUU-3’

5’-ACUUGUAGGUGUUUAAGAA-3’

5’-GGUUAGCCCUGCCUGAAUC-3’

5’-UGUAGGUGUUUAAGAAUUG-3’

RalA:

5’-GGACUACGCUGCAAUUAGA-3’

5’-GCAGACAGCUAUCGGAAGA-3’

5’-GAAAUUCGAGCGAGAAAGA-3’

5‘-GAGCUAAUGUUGACAAGGU-3’

RalB:

5’-GAAAGAUGUUGCUUACUAU-3’

5’-GAAAUCAGAACAAAGAAGA-3’

5’-UACCAAAGCUGACAGUUAU-3’

5’-AGACAAGAAUGGCAAGAAA-3’

Exo70:

5’-GGUUAAAGGUGACUGAUUAUU-3’

5’-GACCUUCGACUCCCUGAUAUU-3’

5’-CUAAGCACCUAUAUCUGUAUU-3’

5’-CGGAGAAGUACAUCAAGUAUU-3’

Sec3:

5’-GAAAUUAACUGGAUCUACU-3’

5’-GUAAAGUCAUUAAGGAGUA-3’

5’-GAAUGUAGCUCUUCGACCA-3’

5’-GAUUAUUUAUCCCGACUAU-3’

Sec8:

5’-GAAUUGAGCAUAAGCAUGU-3’

5’-UAACUGAGUACUUGGAUAU-3’

5’-GCCGAGUUGUGCAGCGUAA-3’

5’-ACUGAGUGACCUUCGACUA-3’

Sec10:

5’-GAAGUCCGAUGCAGAGCAA-3’

5’-GGAGAUACCUUAUGACACA-3’

5’-GGAAAGAAUUAGACAGCGU-3’

5’-CAUUAGGAGUGGAUCGGAA-3’

Sec15:

5’-GAAGUUUGGUGAAUGGUAU-3’

5’-GUUGAUGGCUAUAGAAGAU-3’

5’-GAUAGAGACAGUCGUGAAA-3’

5’-CCAAACUCCGUGAGGAUAU-3’

SUPPLEMENTAL REFERENCES

Balakireva, M., Rosse, C., Langevin, J., Chien, Y.C., Gho, M., Gonzy-Treboul, G., Voegeling-Lemaire, S., Aresta, S., Lepesant, J.A., Bellaiche, Y., *et al.* (2006). The Ral/exocyst effector complex counters c-Jun N-terminal kinase-dependent apoptosis in Drosophila melanogaster. Mol Cell Biol *26*, 8953-8963.

Bampton, E.T., Goemans, C.G., Niranjan, D., Mizushima, N., and Tolkovsky, A.M. (2005). The dynamics of autophagy visualized in live cells: from autophagosome formation to fusion with endo/lysosomes. Autophagy *1*, 23-36.

Cascone, I., Selimoglu, R., Ozdemir, C., Del Nery, E., Yeaman, C., White, M., and Camonis, J. (2008). Distinct roles of RalA and RalB in the progression of cytokinesis are supported by distinct RalGEFs. EMBO J *27*, 2375-2387.

Chien, Y., Kim, S., Bumeister, R., Loo, Y.M., Kwon, S.W., Johnson, C.L., Balakireva, M.G., Romeo, Y., Kopelovich, L., Gale, M., Jr., *et al.* (2006). RalB GTPase-mediated activation of the IkappaB family kinase TBK1 couples innate immune signaling to tumor cell survival. Cell *127*, 157-170.

Dietzl, G., Chen, D., Schnorrer, F., Su, K.C., Barinova, Y., Fellner, M., Gasser, B., Kinsey, K., Oppel, S., Scheiblauer, S., *et al.* (2007). A genome-wide transgenic RNAi library for conditional gene inactivation in Drosophila. Nature *448*, 151-156.

Hsu, S.C., Ting, A.E., Hazuka, C.D., Davanger, S., Kenny, J.W., Kee, Y., and Scheller, R.H. (1996). The mammalian brain rsec6/8 complex. Neuron *17*, 1209-1219.

Kee, Y., Yoo, J.S., Hazuka, C.D., Peterson, K.E., Hsu, S.C., and Scheller, R.H. (1997). Subunit structure of the mammalian exocyst complex. Proc Natl Acad Sci U S A *94*, 14438-14443.

Liang, C., Feng, P., Ku, B., Dotan, I., Canaani, D., Oh, B.H., and Jung, J.U. (2006). Autophagic and tumour suppressor activity of a novel Beclin1-binding protein UVRAG. Nat Cell Biol *8*, 688-699.

Matern, H.T., Yeaman, C., Nelson, W.J., and Scheller, R.H. (2001). The Sec6/8 complex in mammalian cells: characterization of mammalian Sec3, subunit interactions, and expression of subunits in polarized cells. Proc Natl Acad Sci U S A *98*, 9648-9653.

Mizushima, N., Yamamoto, A., Hatano, M., Kobayashi, Y., Kabeya, Y., Suzuki, K., Tokuhisa, T., Ohsumi, Y., and Yoshimori, T. (2001). Dissection of autophagosome formation using Apg5-deficient mouse embryonic stem cells. J Cell Biol *152*, 657-668.

Mizushima, N., Yamamoto, A., Matsui, M., Yoshimori, T., and Ohsumi, Y. (2004). In vivo analysis of autophagy in response to nutrient starvation using transgenic mice expressing a fluorescent autophagosome marker. Mol Biol Cell *15*, 1101-1111.

Moskalenko, S., Henry, D.O., Rosse, C., Mirey, G., Camonis, J.H., and White, M.A. (2002). The exocyst is a Ral effector complex. Nat Cell Biol *4*, 66-72.

Moskalenko, S., Tong, C., Rosse, C., Mirey, G., Formstecher, E., Daviet, L., Camonis, J., and White, M.A. (2003). Ral GTPases regulate exocyst assembly through dual subunit interactions. J Biol Chem *278*, 51743-51748.

Okazaki, N., Yan, J., Yuasa, S., Ueno, T., Kominami, E., Masuho, Y., Koga, H., and Muramatsu, M. (2000). Interaction of the Unc-51-like kinase and microtubule-associated protein light chain 3 related proteins in the brain: possible role of vesicular transport in axonal elongation. Brain Res Mol Brain Res *85*, 1-12.

Pattingre, S., Tassa, A., Qu, X., Garuti, R., Liang, X.H., Mizushima, N., Packer, M., Schneider, M.D., and Levine, B. (2005). Bcl-2 antiapoptotic proteins inhibit Beclin 1-dependent autophagy. Cell *122*, 927-939.

Radtke, A.L., Delbridge, L.M., Balachandran, S., Barber, G.N., and O'Riordan, M.X. (2007). TBK1 protects vacuolar integrity during intracellular bacterial infection. PLoS Pathog *3*, e29.

Rorth, P. (1998). Gal4 in the Drosophila female germline. Mech Dev *78*, 113-118.

Rosse, C., L'Hoste, S., Offner, N., Picard, A., and Camonis, J. (2003). RLIP, an effector of the Ral GTPases, is a platform for Cdk1 to phosphorylate epsin during the switch off of endocytosis in mitosis. J Biol Chem *278*, 30597-30604.

Spiczka, K.S., and Yeaman, C. (2008). Ral-regulated interaction between Sec5 and paxillin targets Exocyst to focal complexes during cell migration. J Cell Sci *121*, 2880-2891.

Vieira, O.V., Botelho, R.J., Rameh, L., Brachmann, S.M., Matsuo, T., Davidson, H.W., Schreiber, A., Backer, J.M., Cantley, L.C., and Grinstein, S. (2001). Distinct roles of class I and class III phosphatidylinositol 3-kinases in phagosome formation and maturation. J Cell Biol *155*, 19-25.

Yeaman, C. (2003). Ultracentrifugation-based approaches to study regulation of Sec6/8 (exocyst) complex function during development of epithelial cell polarity. Methods *30*, 198-206.

Zhong, Y., Wang, Q.J., Li, X., Yan, Y., Backer, J.M., Chait, B.T., Heintz, N., and Yue, Z. (2009). Distinct regulation of autophagic activity by Atg14L and Rubicon associated with Beclin 1-phosphatidylinositol-3-kinase complex. Nat Cell Biol *11*, 468-476.

Supplementary Table 1

Click here to download Supplemental Figure: FigSet_Supplementary_Table_1.pdf

Transgene	Loss-of-microchaete phenotype (%)				Genetic interaction (pvalue)
	Wild-type	Weak	Middle	Strong	
	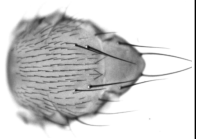	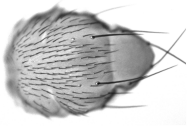	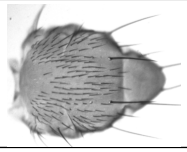	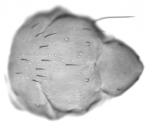	
dsATG1	19	0	0	81	Enhance (p=0.000)
dsATG2	13	15	45	27	No effect (p=0.479)
dsATG6	17	12	22	49	Enhance (p=0.000)
dsATG8a	16	0	19	65	Enhance (p=0.000)
dsATG14L	0	0	0	100	Enhance (p=0.000)
dsVPS34	12	8	38	40	Enhance (p=0.000)
control	14	20	44	22	-

Supplementary Table 1. Genetic interactions between Ral^{35d} and autophagy gene hypomorphs, Related to Figure 1.

Females carrying a scaGAL4 transgene and the Ral^{35d} hypomorphic mutation were crossed with males carrying dsRNA-expressing transgenes targeting the genes indicated in column 1. The loss-of-bristle phenotype of Ral^{35d} males (control) and of Ral^{35d} males expressing the indicated dsRNA under the control of scaGAL4 was analyzed. The distribution of phenotypes in each genetic context is shown. Each distribution was compared to the control distribution using a Chi-Square Goodness-of-Fit test. All distributions are significantly different from control (p value<10E-4), with the exception of dsATG2 (p value=0.48). No bristle phenotype was observed in flies expressing the dsRNAs in absence of Ral^{35d}. Similar genetic interactions were observed when a dominant negative allele of Ral (Ral^{S25N}) was used instead of the Ral^{35d} mutant used here (data not shown).